216

GRAIN-SIZE-YIELD STRESS RELATIONSHIP: ANALYSIS AND COMPUTATION

Marc Andre Meyers, David J. Benson , and Hsueh-Hung Fu
University of California San Diego, Dept. of AMES, La Jolla, CA 92093

ABSTRACT

The seminal contributions of Julia Weertman to our understanding of the mechanical properties of nanocrystalline materials will be brieflyoutlined. A constitutive equation predicting the effect of grain size on the yield stress of metals, based on the model proposed by M. A. Meyers and E. Ashworth (Phil. Mag.46(1982)73), is discussed and extended to the nanocrystalline regime. At large grain sizes, it has the Hall-Petch form, and in the nanocrystalline domain the slope gradually decreases until it asymptotically approaches the flow stress of the grain boundaries. The material is envisaged as a composite, comprised of the grain interior, with flow stress σ_{fB}, and grain boundary work-hardened layer, with flow stress σ_{fGB}. Three principal factors contribute to the grain-boundary hardening:
1.the grain boundaries act as barriers to plastic flow;
2.the grain boundaries act as dislocation sources;
3.elastic anisotropy causes additional stresses in grain-boundary surroundings.
The predictions of this model are compared with experimental measurements over the mono,micro, and nanocrystalline domains. Computational predictions are made of plastic flow as a function of grain size incorporating elastic and plastic anisotropy as well as differences of dislocation accumulation rate in grain boundary regions and grain interiors. This is the first plasticity calculation that accounts for grain size effects in a physically - based manner.

1.INTRODUCTION

Professor Julia Weertman's many scholarly accomplishments before 1990 would clearly place her among the leading materials Scientists worldwide. Her Book (Elementary Dislocation Theory), with Johannes Weertman, has been the standard text on the subject for generations of materials scientists/engineers; it was complemented by her classic review articles in Cahn's Physical Metallurgy. Her early work on fatigue is well recognized and widely cited. However, it is her recent work on nanocrystalline materials, started in 1990, that has captured unanimously the imagination and interest of researchers worldwide. The understanding of the unique mechanical properties of these materials, initiated by Gleiter and coworkers[4, 5], received a very significant contribution from the group led and inspired by Julia Weertman. This work has been published in a series of over twenty papers[6-30]; some of the key features are highlighted below.

Advanced Materials for the 21st Century:
The 1999 Julia R. Weertman Symposium
Edited by Y-W. Chung, D.C. Dunand,
P.K. Liaw, and G.B. Olson
The Minerals, Metals & Materials Society, 1999

The break-down of the classic Hall-Petch dislocation pile-ups in the nanocrystalline regime has been widely discussed. Sample imperfections (voids, microcracks incomplete boundary of particles) masked many of the mechanical characteristics of nanocrystalline materials in early work, and careful processing and characterization has been needed to eliminate (or, at least, mitigate) these effects. Prof. Weertman and her coworkers have played a key role in separating these effects in the past years, and a self-consistent, analytically based knowledge is starting to emerge. The recent overview [30] presents the current thinking on this.

Several mechanisms explaining the strength of nanocrystalline metals have been advanced. In one school of thought, Armstrong and coworkers [31-33] calculated the minimum size of a pile-up and conclude that pile-ups cannot be responsible for the yield stress-grain size effects in the nanocrystalline regime. Koch and coworkers [34-38] studied nanocrystalline iron ; a focused effect was also undertaken to remove sample flaws (voids, microcracks, incomplete boundary of particles, etc.) in order to obtain more reliable mechanical strength under both compression and tension. Scattergood and Koch[35] proposed a micromechanism for plastic deformation. In summary, the experimental results indicate that the Hall-Petch slope in the nanocrystalline domain is lower than in the microcrystalline (conventional) range of grain sizes. In some cases, a zero or even negative Hall-Petch slope has been reported[39].

An alternate mechanism is proposed here. It is essentially an extension of the model proposed by Meyers and Ashworth[40] to the nanocrystalline regime. This model does not require pile-ups at grain boundaries. It is based on earlier ideas advanced by Ashby[41], Hirth[42], and Thompson[43]. Conceptually, it is similar to parallel ideas developed by Margolin[44]. It will be shown that the Meyers-Ashby (MA) model, which has a built-in deviation from a Hall-Petch relationship at small grain sizes, can be successfully extended to the nanocrystalline regime. The concept of a work-hardened grain-boundary layer, essential to the MA model, is modeled computationally, for different grain sizes, and it is shown that similar predictions are obtained.

2.THE MODEL

The model, which is described in detail elsewhere[40], is summarized here. A polycrystalline aggregate, upon being subjected to external tractions, develops a highly inhomogeneous state of internal stresses, due to the elastic anisotropy of the individual grains. Such inhomogeneous state of stress can only be avoided if the anisotropy ratio is one. For instance, for iron , one has:

E_{100}=125 GPa
E_{110}=200 GPa
E_{111}=272 GPa

The compatibility requirement at the grain boundaries create additional stresses, τ_I. Meyers and Ashworth [40] found for nickel that

$$\tau_I = 1.37\ \sigma_{AP} \qquad (1)$$

where σ_{AP} is the applied normal stress. In a uniform, homogeneous natural, $\tau = \sigma/2$. Thus, the shear stress at the interface is between 2 and 3 times the maximum shear stress in a homogeneous/uniform material. It is therefore logical to expect the initiation of plastic flow to take place in the grain boundary regions. Other factors that contribute to this:

a) Grain boundaries are sources of dislocations. This is a well known phenomenon ; grain-boundary ledges and grain-boundary dislocations can initiate plastic deformation (e. g., Li and Chou[45], Murr[46], Sutton and Balluffi[47]).
b) Grain boundaries segregate impurities and foreign atoms and their mechanical properties differ from the grain interiors.
c) Dislocations pileup at grain boundaries.

Figure 1 shows the sequence of stages as the applied stress, σ_{AP}, is increased. As the applied stress increases, a work hardened layer along the grain boundaries is formed. This is eloquently illustrated by Murr and Hecker [48]. This build-up of plastic deformation has been recently also measured by Adams[49]. Once this work hardened grain-boundary layer is formed, the stresses within the polycrystalline aggregate homogenize. Stages a-c in Figure 1 represent the dominance of elastic compatibility strains and the formation of a grain boundary work-hardened layer. Stages d-f represent the response of a composite material, consisting of dislocation-free grain interiors, with a flow stress σ_{fG}, and grain-boundary layers, with a flow stress σ_{fGB}. The flow stress of the aggregate is obtained, in approximate fashion, from:

$$\sigma_y = A_B\sigma_{fB} + A_{GB}\,\sigma_{fGB} \tag{2}$$

A_B and A_{GB} are the areal fraction of grain interior and grain boundary, respectively. Figure 2 shows an idealized representation of the aggregate. Grains are assumed to be spherical, with a diameter D; the grain boundary layers are assumed to have a thickness t (in each grain). The diametral areal fractions are expressed by:

$$A_{GB} = \frac{\frac{1}{4}\pi\left[D^2 - (D-2t)^2\right]}{\frac{1}{4}\pi D^2} \tag{3}$$

$$A_B = \frac{\frac{1}{4}\pi(D-2t)^2}{\frac{1}{4}\pi D^2} \tag{4}$$

Substituting (3) and (4) into (2):

$$\sigma_y = \sigma_{fB} + 4\left(\sigma_{fGB} - \sigma_{fB}\right)tD^{-1} - 4\left(\sigma_{fGB} - \sigma_{fB}\right)t^2D^{-2} \tag{5}$$

Different sections, marked S_1, S_2, S_3, S_4, and S_5 in Figure 2b, produce different areal fractions A_B and A_{GB}. Meyers and Ashworth [40] estimated the mean values of t and D, $\bar{t}$ and $\overline{D}$, respectively. They are:

$$\overline{D} = \frac{\pi}{4}D \tag{6}$$

$$\bar{t} = 1.57t$$

Hence, it is more correct to use these values. The ratio tD^{-1} is approximately equal to $2\bar{t}\,\overline{D}^{-1}$. Equation 5 breaks down when D≤2t. The Hall-Petch dependency, universally obtained for large grain sizes, can be inserted into Eqn. (5) by establishing a functional dependence of t of the form:

$$t = k_{MA}D^{1/2} \tag{7}$$

Substituting Eqn. (7) into a modified form of Eqn. (5) to take Eqns. (6) into account:

$$\sigma_y = \sigma_{fB} + 8k_{MA}\left(\sigma_{fGB} - \sigma_{fB}\right)\overline{D}^{-1/2} - 16k_{MA}{}^2\left(\sigma_{fGB} - \sigma_{fB}\right)\overline{D}^{-1} \qquad (8)$$

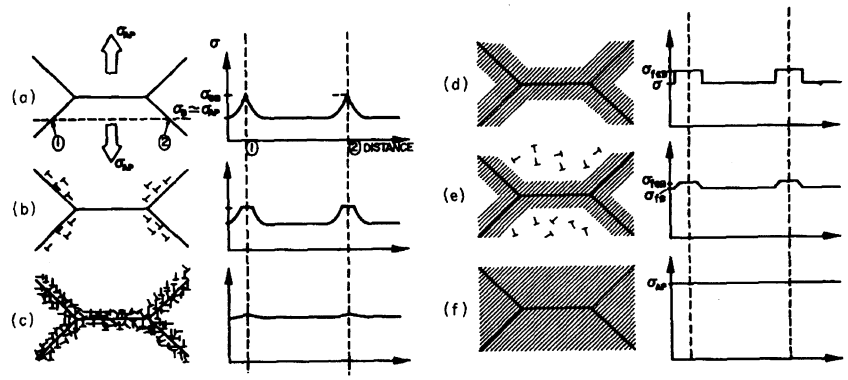

Figure 1: Sequence of stages in polycrystalline deformation, starting with (a, b) localized plastic flow in the grain-boundary regions (microyielding), forming a grain-boundary work-hardened layer (c, d) that effectively reinforces the microstructure, and leading to (e, f) macroyielding in which the bulk of the grains undergo plastic deformation. (from Meyers and Ashworth [40])

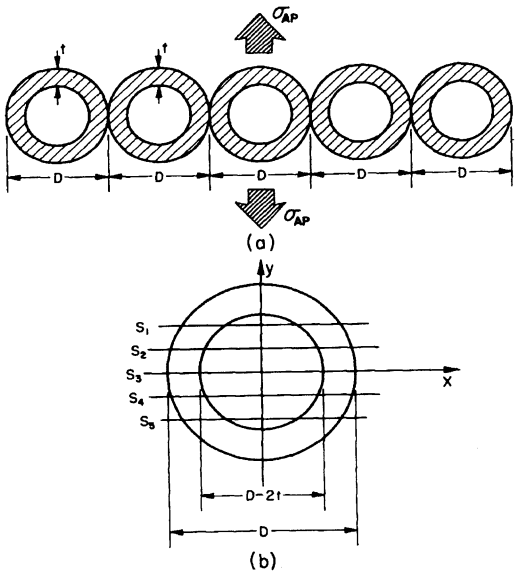

Figure 2: (a) Polycrystalline aggregate viewed as composite material composed of bulk and grain-boundary material, with flow stresses σ_{GB} and σ_{fGB} respectively. (b) Idealized spherical grain of diameter D with grain-boundary layer of thickness t; sections S_1, S_2, S_3, S_4, and S_5, reveal different proportions between the areas of the bulk and grain-boundary material. (from Meyers and Ashworth [40])

For large grain sizes (the micrometer range) the $D^{-1/2}$ term dominates and a Hall-Petch relationship is obtained. The Hall-Petch slope, k_{HP}, is equal to:

$$k_{HP} = 8k_{MA}(\sigma_{fGB} - \sigma_{fB}) \quad (9)$$

As the grain size is decreased, the D^{-1} term becomes progressively dominant, and the σ_y vs $D^{-1/2}$ curve goes through a maximum. This occurs at:

$$D_c = (4k_{MA})^2 \quad (10)$$

For values of $D < D_c$, it is assumed that the flow stress reaches a plateau.

3.ANALYTICAL PREDICTIONS AND COMPARISON WITH EXPERIMENTS

The predictions of Eqn. 8 are compared with the best experimental results available in the literature , to the authors' knowledge. Yield stresses for nanocrystalline Fe and Cu, reported by Mallow and Koch[37], and Weertman et al.[30], respectively, are shown in Figure 3. The experimental results in the nanocrystalline range are complemented by Hall-Petch slopes in the microcrystalline range. These slopes are reported in the literature. For iron, experimental results reported by Armstrong [50] were used. For copper, experimental results by Feltham and Meakin[51] and Andrade et al. [52] are used. There are other experimental results in the literature, that fall in the range reported in Figure 3. For iron, Abrahamson[53] carried out experiments in the lower range of the conventional Hall-Petch and started to observe a deviation from the accepted slope. Two experimental points from Abrahamson[53] are shown in Figure 3a; the Hall –Petch slope starts to decrease.

It is clear, for both Fe and Cu, that the σ_y vs $D^{-1/2}$ relationship is not linear over the range millimeter-nanometer. The Hall-Petch line is an approximation that is effective in the mm-μm range. There is strong evidence that the slope decreases and that the curve asymptotically approaches a plateau when the grain size is progressively reduced. Equation 8 is successful in representing the principal features experimentally observed. Three parameters have to be established: σ_{fB}, σ_{fGB}, and k_{MA}. σ_{fB} is the saturation stress and represents the flow stress of the work hardened grain-boundary layer. It is taken as the maximum of the yield stress. k_{MA} is obtained by conversion of k_{HP} according to Eqn. 9. This ensures a good match between HP and MA for large grain sizes. Table 1 shows the parameters used in the calculation. The continuous curves in Figure 3 represent the application of Eqn. 8; a reasonable fit is obtained and the principal features are captured. For grain sizes below the maximum of the flow stress in the MA equation, a straight horizontal line is taken; in this regime, the grain boundaries (σ_{fGB}) dominate the process.

Table 1 Parameters used for MA model

	σ_{fB} (MPa)	σ_{fGB} (MPa)	k_{HP} (MPa $m^{1/2}$)	k_{MA} ($m^{1/2}$)
Fe	100	2800	0.48	2.2×10^{-5}
Cu	25	900	0.112-0.172	$(1.6\text{-}2.4) \times 10^{-5}$

There are many simplifications and assumptions in this model. The most prominent are:

a) The work hardened layer t is assumed to have a grain size dependence of $D^{-1/2}$. This assumption is based on the σ_y vs. $D^{-1/2}$ dependence.

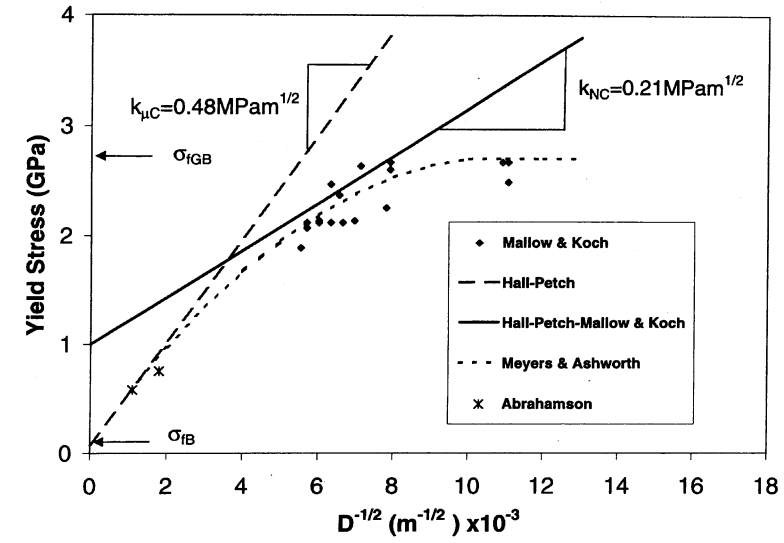

(a)

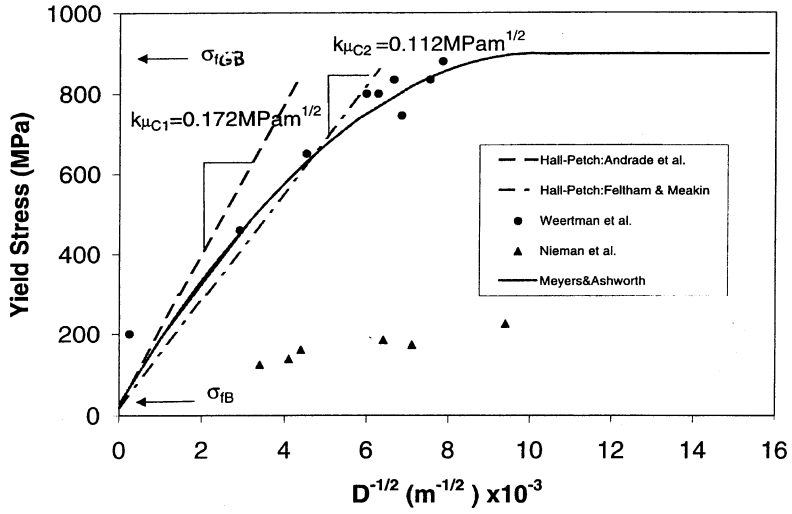

(b)

Figure 3: σ_y vs. $D^{-1/2}$ relationship for (a) iron and (b) copper; comparison of experimental results and predictions of Equation 8.

b) The flow stress of this layer is constant. In reality, a gradient of work hardening is expected.

c) The grain boundary flow stress reaches the saturation value σ_{fGB} at an early level of global plastic strain.

In spite of these drastic assumptions, a good fit is obtained and it is felt that the model captures the key physical features. It should be noted that Gertsman et al. [54] obtained experimentally a similar decrease in the Hall-Petch slope for copper, in the nanocrystalline range. However, the yield stresses are significantly lower than the latest results by Weertman et al. [30]. Differences can be attributed to improved processing methods. Figure 3b also shows (▲)earlier experimental data by Nieman et al.[7]. These results illustrate how much processing can affect the strength of nanocrystalline materials. These results were not used in the modeling effort.

4.COMPUTATIONAL APPROACH

4.1 Description of code

The finite difference community has used Eulerian methods for over thirty years to analyze problems with explosive loading, but until comparatively recently, they were too computationally demanding and inaccurate to be attractive for solving problems in solid mechanics. The strengths and weaknesses of the Eulerian formulation are summarized in a brief description of the computational methods used in *Raven*, an explicit, multi-material Eulerian program developed by Benson. A comprehensive review paper by Benson [55] discusses the algorithms in greater detail.

Operator splitting replaces a differential equation with a set of equations that are solved sequentially. This strategy is formally limited to second order accuracy [56], which is achieved in practice. While the first strategy does not have this theoretical limitation, it rarely achieves better than first order accuracy in multi-material formulations. A generic transport equation is

$$\frac{\partial \varphi}{\partial t} + \vec{u} \cdot \nabla \varphi = \Phi \tag{11}$$

where φ is a solution variable, $\vec{u}$ is the velocity, and Φ is a source term. This equation is split into

$$\frac{\partial \varphi}{\partial t} = \Phi \tag{12}$$

$$\frac{\partial \varphi}{\partial t} + \vec{u} \cdot \nabla \varphi = 0 \tag{13}$$

where Eqn. (12) and Eq. (13) are referred to as the Lagrangian and Eulerian steps respectively. The Lagrangian step uses the central difference algorithm to advance the solution in time in the same manner as a standard explicit Lagrangian finite element formulation.

The elements are four node quadrilaterals with one point integration and a viscous hourglass control. Hourglass modes may stop Lagrangian calculations performed with uniformly reduced integration by turning the elements inside out. Since the hourglass modes are orthogonal to the strain field, the stresses in the elements are unaffected by the modes. The Eulerian formulation is immune to the mesh distortion problem, but the hourglass viscosity is included to filter out the diamond pattern the hourglass modes introduce into the contours of the velocity field.

The transport calculation is equivalent to a projection of the solution from one mesh onto another, and a perfect projection should be completely conservative. Most transport algorithms are conservative by construction: a flux added to one element is subtracted from its neighbor.

van Leer[56] developed the MUSCL transport algorithm used in the current calculation. The transport volumes are geometrical calculations defined by the mesh motion and they are independent of the transport kernel. The one-dimensional algorithm is extended to two dimensions by performing sweeps along one mesh direction, then another sweep in the other direction.

4.2 Results of Computations

For computational calculations, realistic polycrystals were used and are shown in Figure 4. Four grain sizes were modeled: 100, 10 , 1, and 0.1 μm. The thickness of the grain-boundary layer, t, was varied and the respective values used are: 3.75, 0.75, 0.15, and 0.03 μm. The material chosen for the modeling effort is copper, because of the significant amount of information on grain-size effects available(see Figure 3b). The microstructures, already divided into grain interiors and grain-boundary layers, are shown in Figure 4. For the largest grain size modeled (100 μm) , the grain–boundary region is barely distinguishable, whereas for the smallest grain size (0.1 μm) , the grain–boundary region occupies a significant portion. An optimum grain-boundary configuration and grain structure are still being developed, as seen by the differences between Figs. 6(a,c) and 6(b,d). The different mechanical response of the two regions was also incorporated. The grain-boundary region was considered to be highly work hardened, whereas the grain interiors were modeled as monocrystals. At the present stage, no attempt was made to incorporate elastic incompatibility stesses and the build-up of plastic deformation into thre model; this will be done at a later stage[57]. The model has the capability of incorporating as many as fifteen different crystallographic directions (manifested by different mechanical responses) .This is indicated by the different shades of gray in Figure 4. However, at the present stage all grain interiors were assumed to have the same (monocrystalline) response; the same assumption was made for the grain-boundary layers. The crystallographic orientation and specimen dimensions have a profound effect on the mechanical response of monocrystals . The response of annealed monocrystal and work-hardened polycrystal are shown in Figure 5. The monocrystal data is based on experimental results reported by Diehl [58]and represents an average; a bilinear stress-strain response is assumed(Fig. 5a) that captures both the easy glide and linear hardening stages of work hardening. Then work-hardened grain-boundary region was assumed to respond as a perfectly plastic material with a flow stress of 900 MPa (this value is identical to the one from Table 1). These two stress-strain responses were incorporated into the code Raven and calculations were successfully carried out. The results of one calculation for a grain size of 0.1 μm are shown in Figure 6. The results are presented at three levels of plastic strain; 0.05, 0.02, and 0.03. The evolution of stress can be clearly followed in the sequence shown in Figs. 6a, b, and c. Figure 6d shows the computed stress-strain curve. The stresses rise rapidly in the grain-boundary region, while they remain low in the grain interiors (lighter gray indicates a higher stress). As plastic deformation progresses, the interiors of the grains gradually work harden, and the stress differential decreases. This is shown in Fig. 6c; the shades of gray in grain–boundary regions and grain interiors become less distinct. The stress-strain response is shown in Fig. 6d. The material exhibits a pseudo-elastic regime with a flow stress of approximately 270 MPa. This response is very similar to the one experimentally reported by Nieman et al. [7].

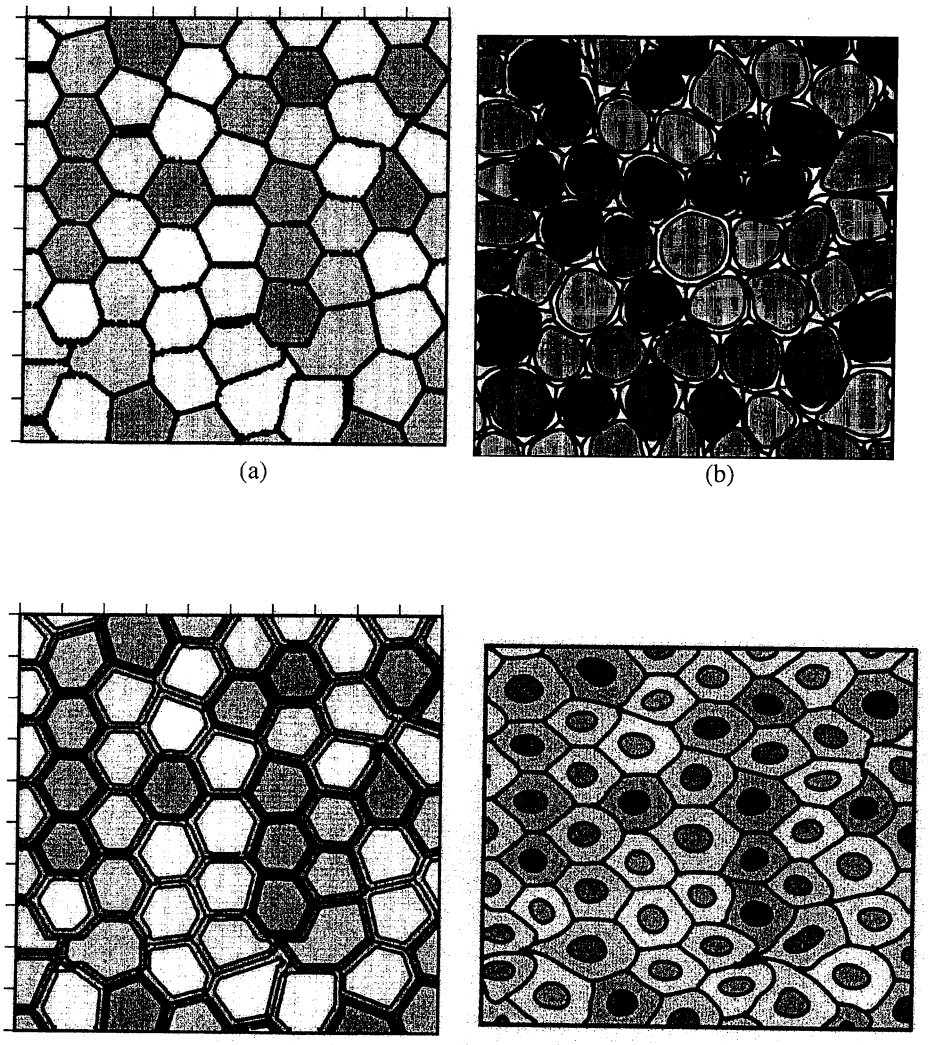

Figure 4: Simulated polycrystalline aggregate used in computations; (a) D=100μm, t=3.75 μm; (b) D =10μm, t=0.75μm; (c) D=1μm, t=0.15 μm; (d) D=0.1 μm, t= 0.03 μm

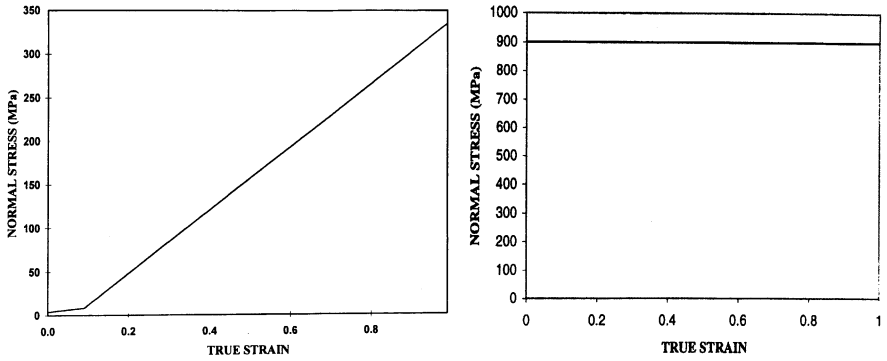

(a) (b)

Figure 5: Stress-strain curves for (a)monocrystalline copper representing grain interior and (b) work-hardened copper, corresponding to the grain-boundary region.

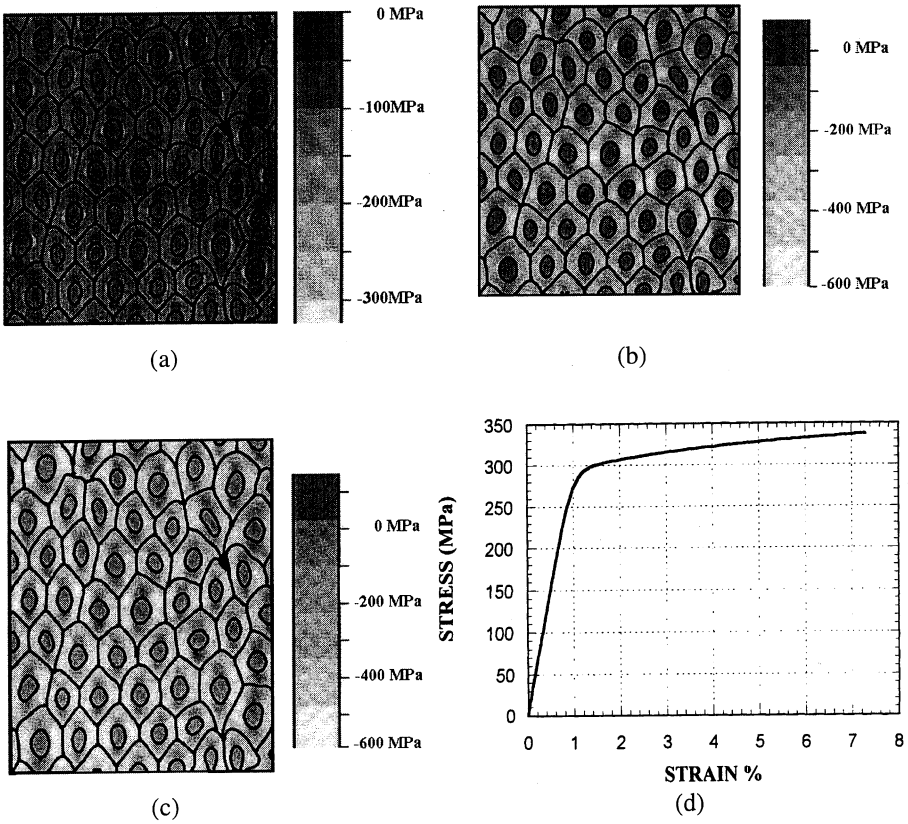

(a) (b)

(c) (d)

Figure 6: (a-c) Deformation sequence in specimen with grain size of 0.1μm (d) Computed stress-strain curve.

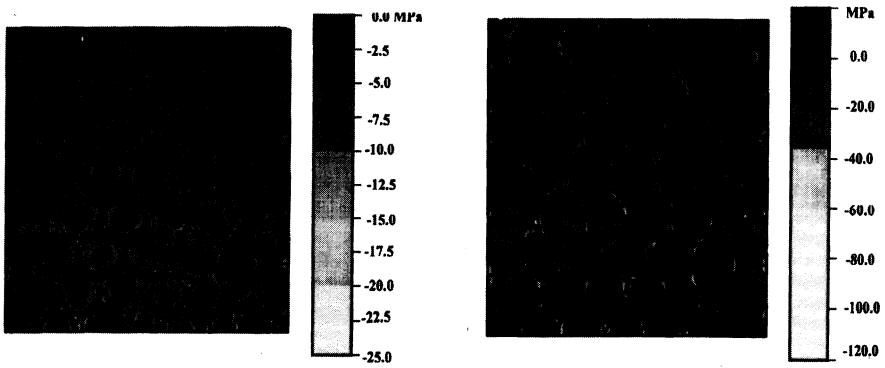

(a) (b)

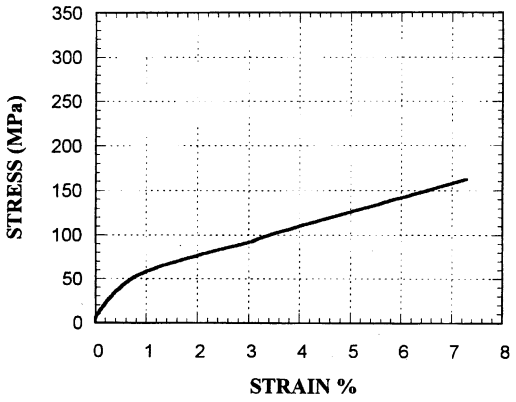

(c)

Figure 7:(a,b)Deformation sequence in specimen with grain size 10 μm; (c) Computed stress strain curve.

Figure 7 shows the deformation sequence and computed stress-strain curve for the grain size of 10 μm. The stresses are higher in the grain boundary region (lighter shading in Figure 7(a)) and gradually increase in the grain interiors, as they work harden(Figure 7(b)). The stress-strain curve is significantly different from the one in Fig 6c; the material has a much lower flow stress. It is interesting to notice that these computations predict an "apparent" elastic regime with a slope that is a fraction of Young's modulus . This is due to the interaction between the two regions. Thus, the lower elastic moduli observed for nanocrystalline materials could be attributed to these effects. No elastic deformation was incorporated into the mechanical responses modeledin Figs.6 and 7.

5.CONCLUSIONS

It was proposed by Meyers and Ashworth [40] that elastic anisotropic effects in polycrystals are responsible for the formation of a work hardened layer along the grain boundaries, early in the microplastic region . This grain boundary work-hardened layer becomes increasingly important as the grain size is decreased. Polycrystals are modeled (both analytically and computationally) as a composite of a work-hardened boundary layer surrounding grain interiors comprised of an annealed material having a essentially monocrystalline response. The analytical predictions using this framework are successfully extended from the micro to the nanocrystalline domain and show a good correlation with experimental results for copper and iron. The decrease of the Hall-Petch slope in the nanocrystalline domain is captured and corresponds to a grain size for which the thickness of the work hardened layer is equal to one half the grain diameter. Computational predictions using the Eulerian code Raven successfully produce stress-strain curves of the polycrystalline aggregates and predict the correct trend in grain sizes .

ACKNOWLEDGMENT

This research was supported by the U.S. Army Research Office Multidisciplinary University Research Initiative (Contract No. DAAH 04-96-1-0376).

REFERENCES

1.J. Wertman and J. R. Weertman, "Elementary Dislocation Theory", MacMillan, 1964.
2.J. Weertman and J. R. Weertman, "Mechanical Properties, Mildly Temperature Dependent" in " Physical Metallurgy" , R. W. Cahn, ed., North Holland, Amsterdam, 1970, Chapter 15, p.921.
3.J. Weertman and J. R. Weertman, "Mechanical Properties, Strongly Temperature Dependent" in " Physical Metallurgy' , R. W. Cahn, ed. ,North Holland, Amsterdam, 1970, Chapter 16, p.983.
4.R. Birringer, H. Gleiter, H.-P. Klein, and P. Marquardt, "Nanocrystalline Materials An Approach to A Novel Solid Structure With Gas-like Disorder?", Phys. Lett., 102A(1984) 365-369.
5.H. Gleiter, "Nanostructured Materials: State of the Art and Perspectives", Z. fur Metallkunde, 86(1995) 78-83.
6.G.W. Nieman, J.R. Weertman, R.W. Siegel, "Tensile Strength and Creep Properties of Nanocrystalline Palladium," Scripta Metallurgica et Materialia, 24(1990), 145-150.
7.G.W. Nieman, J.R. Weertman, R.W. Siegel, "Mechanical Behavior of Nanocrystalline Cu and Pd," Journal of Materials Research, 6(1991), 1012-1027.

8.G.E. Fougere, J.R. Weertman, R.W. Siegel, S. Kim, "Grain-Size Dependent Hardening and Softening of Nanocrystalline Cu and Pd," Scripta Metallurgica et Materialia, 26(1992), 1879-1883.
9.J.R. Weertman, "Hall-Petch Strengthening in Nanocrystalline Metals," Materials Science and Engineering A, 166(1993), 161-167.
10.J.R. Weertman, D. Farkas, K. Hemker, H. Kung, M. Mayo, R. Mitra, H. Van Swygenhoven, "Structure and Mechanical Behavior of Bulk Nanocrystalline Materials," MRS Bulletin, 24(1999), 44-50.
11.R. Weertman, P.G. Sanders, "Plastic Deformation of Nanocrystalline Metals", Diffusion and Defect Data Part B (Solid State Phenomena) Diffusion," Defect Data B, Solid State Phenom, 35-36(1994), 249-62.
12.G.E. Fougere, J.R. Weertman, R.W. Siegel, "Processing and Mechanical Behavior of Nanocrystalline Fe," Nanostruct. Mater., 5(1995), 127-3
13. P.G. Sanders, A.B. Witney, J.R. Weertman, R.Z. Valiev, R.W. Siegel, "Residual Stress, Strain and Faults in Nanocrystalline Palladium and Copper," Mater. Sci. Eng. A., A204(1995), 7-11.
14. G.E. Fougere, L. Riester, M. Ferber, J.R. Weertman, R.W. Siegel, "Youngÿs Modulus of Nanocrystalline Fe Measured by Nanoindentation," Mater. Sci. Eng. A, A204(1995), 1-6.
15.A.B. Witney, P.G. Sanders, J.R. Weertman, J.A. Eastman, "Fatigue of Nanocrystalline Copper," Scr. Metall. Mater., 33(1995), 2025-30.
16.M.N. Rittner, J.R. Weertman, J.A. Eastman, "Structure-Property Correlations in Nanocrystalline Al-Zr Alloy Composites," Acta Mater., 44(1996), 1271-86.
17.P.G. Sanders, J.R. Weertman, J.G. Barker, "Structure of Nanocrystalline Palladium and Copper Studied by Small Angle Neutron Scattering," J. Mater. Res., 11(1996), 3110-20.
18.P.G. Sanders, M. Rittner, E. Kiedaisch, J.R. Weertman, H. Kung, Y.C. Lu, "Creep of Nanocrystalline Cu, Pd, and Al-Zr," Nanostruct. Mater.,9 (1997), 433-40.
19.M. Eldrup, P.G. Sanders, J.R. Weertman, "Positron Annihilation Study of the Influence of Grain Size And Purity on the Annealing Behaviour of Nano-Crystalline Copper," Mater. Sci. Forum, 255-257(1997), 436-8.
20.P.G. Sanders, G.E. Fougere, L.J. Thompson, J.A. Eastman, J.R. Weertman, "Improvements in the Synthesis and Compaction of Nanocrystalline Materials," Nanostruct. Mater., 8(1997), 243-52.
21.P.G. Sanders, C.J. Youngdahl, J.R. Weertman, "The Strength of Nanocrystalline Metals with and without Flaws," Mater. Sci. Eng. A, Prop., 234-236(1997), 77-82.
22.C.J. Youngdahl, P.G. Sanders, J.A. Eastman, J.R. Weertman, "Compressive Yield Strengths of Nanocrystalline Cu and Pd," Scr. Mater., 37(1997), 809-13.
23.M.N. Rittner, J.R. Weertman, J.A. Eastman, K.B. Yoder, D.S. Stone, "Mechanical Behavior of Nanocrystalline Aluminum-Zirconium," Mater. Sci. Eng. A, Prop., 237(1997), 185-90.
24.P.G. Sanders, J.A. Eastman, J.R. Weertman, "Elastic and Tensile Behaviour of Nanocrystalline Copper and Palladium," Acta Mater., 45(1997), 4019-25.
25.Z. Huang, L.Y. Gu, J.R. Weertman, "Temperature Dependence of Hardness of Nanocrystalline Copper in Low-Temperature Range," Scr. Mater., 37(1997), 1071-5.
26.S.R. Agnew, J.R. Weertman, "The Influence of Texture on the Elastic Properties of Ultrafine-Grain Copper," Mater. Sci. Eng. A, Prop. 242(1998), 174-80.
27.S.R. Agnew, J.R. Weertman, "Cyclic Softening of Ultrafine Grain Copper," Mater. Sci. Eng. A, A244(1998), 145-53.
28.P.G. Sanders, J.A. Eastman, J.R. Weertman, "Pore Distributions in Nanocrystalline Metals from Small-Angle Neutron Scattering," Acta Mater., 46(1998), 4195-202.
29.T. Ungar, S. Ott, P.G. Sanders, A. Borbely, J.R. Weertman, "Dislocations, Grain Size and Planar Faults in Nanostructured Copper Determined by High Resolution X-Ray Diffraction and A New Procedure of Peak Profile Analysis," Acta Mater., 46(1998), 3693.

30.J.R. Weertman, D. Farkas, K. Hemker, H. Kung, M. Mayo, R. Mitra, H. Van Swygenhoven, Structure and Mechanical Behavior of Bulk Nanocrystalline Materials, MRS Bulletin, Feb, , 24(1999):44-50.

31.R.W. Armstrong and T.R. Smith, in "Processing and Properties of Nanocrystalline Materials", eds. C. Suryanarayana, PA, 1996, 0.345.
32.C.S. Pande, R.A. Masamura, and R.W. Armstrong, Nanostr. Mat., 2(1993) 323.
33.T.R. Smith, R.W. Armstrong, P.M. Hazzledine, R. A. Masamura, And C.S. Pande, "Pile-up Based Hall-Petch Considerations at Ultrafine Grain Sizes", in " Grain Size and Mechanical Properties –Fundamentals and Applications", MRS, Boston, MA, 1995, 31-37.
34.J.S. C. Jang and C.C. Koch, Scripta Mat., 24(1990) 1599.
35.R.O. Scattergood and C.C. Koch, Scripta Met., 27 (1992) 1195.
36.T.R. Mallow and C.C. Koch, Acta Mater., 45(1997) 2177-2186.
37.T.R. Mallow and C.C. Koch, "Mechanical properties, Ductility, and Grain Size of Nanocrystalline Iron Produced by Mechanical Attrition", Met. And Mat. Trans., 29A(1998) 2285-2295.
38.C.C. Koch, D.G. Morris, K.Lu, and A. Inoue, "Ductility of Nanostructureed Materials", MRS Bulletin, 24(1999) N0.2 55-58.
39.A.H. Chokshi, A.S. Rosen, J. Karch, and H. Gleiter, Scripta Met., 23(1989) 1679.
40.M.A. Meyers and E. Ashworth, "A Model for the Effect of Grain Size on the Yield Stress of Metals", Phil. Mag., A 46(1982) 737-759
41.M. F. Ashby, Phil. Mag. 21(1970)399-424
42.J. P. Hirth, Met. Trans. 3(1972)n 161-185.
43.A. W. Thompson, in "Work Hardening in Tension and Fatigue", ed. A. W. Thompson, AIME, 1977, 399-424.
44.H. Margolin, "Polycrystalline Yielding-Perspectives on its Onset", Acta Mat., 46(1998) 6305-6309.
45.J.C.M. Li and Y.T. Chou, Metall. Trans., 1(1970) 1145.
46.L.E. Murr, "Interfacial Phenomena in Metals and Alloy", Addison Wesley, Reading, MA, 1975.
47.A.P. Sutton and R.F. Baluffi, "Interfaces in Crystalline Materials", Oxford Univ. Press, NY, 1994 .
48.L. E. Murr and S.S. Hecker, Scripta Met., 13(1979) 667
49.B. Adams, Private communication, 1999.
50.R.W. Armstrong, "The Influence of Polycrystal grain size on Mechanical Properties", in "Advances in Materials Research" , Herman, 4(1970) 101.
51.P. Feltham and J.D. Meakin, Phil. Mag. 2(1957) 105.
52.M.A. Meyers, U.R. de Andrade, and A.H. Chokshi, "The Effect Of Grain Size On The High Strain, High Strain Rate Behavior Of Copper" 26A(1995) 2881-2893.
53.E.P. Abrahamson, II, in "Surface and Interfaces", Syracuse Univ. Press, 1968, p.262.
54.V.Y. Gertsman, M. Hoffmann, H. Gleiter and R. Birringer, "The Study of Grain Size Dependence of Yield Stress of Copper for a Wide Grain Size Range", Acta Mat., 42(1994) 3539-3544.
55.D. J. Benson ,Comp. Meth. Appl. Mech. Engng. 999(1992) 235-394.
56.B. van Lee, J. Comp. Phys. 23 (1977)276-299.
57.M. A. Meyers, D. J. Benson, and H.-H. Fu, in preparation, (1999).
58.J. Diehl, Z. Metallk., 47 (1956)331.